Fourier-transformed infrared absorption spectroscopy: a tool to characterize the chemical composition of Ar-NH3-SiH4 dielectric barrier discharge

Julien Vallade, Françoise Massines

Fourier-transformed infrared absorption spectroscopy: a tool to characterize the chemical composition of $Ar–NH_3–SiH_4$ dielectric barrier discharge

Julien Vallade[1,2] and Françoise Massines[1]

[1]PROMES, CNRS, Laboratoire Procédés, Matériaux et Énergie Solaire, Tecnosud, Rambla de la Thermodynamique, 66100 Perpignan, France.

[2] ADEME, French Environment and Energy Management Agency, 20, avenue du Grésillé, BP 90406, 49004 Angers Cedex 01, France.

ABSTRACT. This study brings initial insight on the characterization of the gas chemical composition in a dielectric barrier discharge by Fourier-Transformed InfraRed (FTIR) absorption spectroscopy. Capitalizing on a double path of the IR beam, measurements were performed in 5 cm-long, 2 mm-gap plasma. As the IR beam cross-section in the plasma was 2x2 mm², a translation system was used to scan the plasma along the direction of the gas flow with a 2 mm spatial resolution.
In the case of $Ar–SiH_4$(67ppm)–NH_3(133ppm) glow-mode DBD, all IR spectra peaks from 6000 to 800 cm^{-1} are related to vibrations of Si-H from SiH_4 and N-H from NH_3. Here, the N-H vibration is observable but non-quantifiable.
At 50 kHz excitation, the absolute concentration of SiH_4 was measured on different positions and different power values in continuous and modulated modes. In the absence of powder formation in the plasma and for an initial density of $1.6.10^{15}cm^{-3}$, all the measurements are fitted by the same exponential decay leading to an energy of 42eV per dissociated molecule of SiH_4. The presence of powders in the plasma reduces SiH_4 dissociation rate by a factor larger than 4.

Keywords: Dielectric barrier discharge, atmospheric pressure glow discharge, Fourier-transformed infrared absorption, silane decomposition, plasma chemistry.

1. INTRODUCTION

Dielectric barrier discharge (DBD) offers a robust solution for getting non-equilibrium atmospheric pressure plasma [1]. In more and more applications such as thin-film deposition, surface treatment, pollutant remediation and sterilization [2], DBD is used to initiate chemistry at low temperature. Knowing how gas chemical composition evolves as a function of position and time is vital for firmly controlling the plasma process and understanding the discharge behavior. DBD non-invasive characterization tools are limited. High pressure poses challenges for methods like mass spectrometry that work under vacuum or for method using probes restricting their size to sub-micrometer range in order not to disturb the plasma. The dielectric also complicates electrical current and voltage measurements, and the small size of the gap narrows the potential panel of convenient diagnostic tools. Optical methods are often the most useful. Among them, optical emission spectroscopy (OES) [7] has

emerged as the most common technique. Its main limitation comes from the fact that light intensity is related not only to the density of the emissive species but also to their excitation, and in DBD the excitation mechanism is often the dominant one. This problem is avoided by using absorption techniques such as cavity ring-down spectroscopy [10], one or two photons laser-induced fluorescence [11]-[13], or IR tunable diode laser absorption spectroscopy [14]. The major setback of these characterizations is their limited spectral range, which means they provide information on the density of only one chemical species at a time. Moreover, both laser and OES-based techniques can only yield data on atoms or small molecules. A useful spectroscopy method to scan a very large range of molecules is the Fourier-Transform InfraRed (FTIR) spectroscopy. The feasibility of using a Fourier transform spectrometer to take IR absorption measurements on a dielectric barrier discharge has very recently been demonstrated [15]. The aim of this work is to better evaluate the potential of using FTIR absorption to characterize gas chemical composition variation in a DBD.

The studied gas is a mixture of argon, 133 ppm of ammonia and 67 ppm of silane. This specific chemical composition was chosen because it is the most convenient to make antireflective silicon nitride coating on crystalline silicon solar cell [16]. After a detail presentation of the IR optical set-up and the method to get absolute values of SiH_4 concentration, results as a function of the position in the plasma and the power will be detailed. Thus the influence of power modulation and powder formation will be discussed.

2. MATERIALS AND METHODS

This section starts by presenting the plasma reactor and discharge cell, then goes on to describe the FTIR spectroscopy optical setup and the solution adopted to optimize background acquisition and calibration to get absolute concentrations.

2.1. Plasma reactor

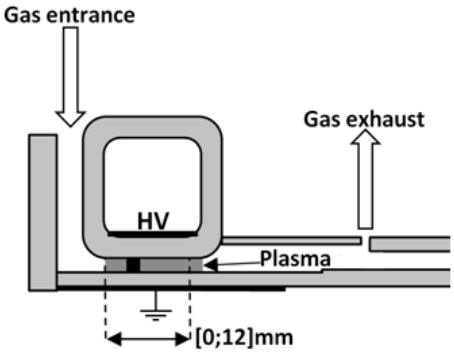

Figure 1 : Schematic illustration of the discharge cell configuration. The dark square in the plasma zone depicts the 2 by 2 mm² IR beam. Beam position is varied from 0 to 12 mm.

Figure 1 gives a schematic illustration of the discharge cell. Since the discharge is a DBD, the plasma is located between two dielectric surfaces: the bottom of an alumina barrel 3 mm thick with a metalized inner surface (14 by 50 mm²) and an alumina plate also 3 mm thick with a metalized rear face (150 by 70 mm²). The voltage is applied across the metal layers deposited on the barrel and the plate. The gas is injected on one side of the gap through a 50 mm by 2 mm linear slit, and guided by potassium bromide (KBr) blades up to the gas exhaust system. This configuration enables uniform gas distribution throughout the 50 mm depth of the plasma. The discharge cell is inside a closed reactor which is pumped to remove air before being filled with argon up to 10^5 Pa. The gas is composed of argon (3 L/min), ammonia (133 ppm) and silane (67 ppm). The gap between the two electrodes is

2 mm. Plasma excitation is a 50 kHz sinusoidal signal that can be modulated to obtain on/off times of a few milliseconds. These conditions make it easy to obtain a homogeneous-glow DBD free of microdischarge.
The discharge mean power is an important parameter of the process. Its value is calculated according to equation 1. Assuming that the plasma fill all the gas space between the electrodes (1.4cm^3), for this study, the mean power density of the glow DBD ranges from 60 to 800 mW/cm³.

$$P(W) = \frac{1}{T}\int_0^T V_{applied}(V) * I_{mesured}\ (A) \qquad \textbf{Equation 1}$$

2.2. FTIR absorption spectroscopy with 2 mm spatial resolution

2.2.1.Optical setup.

The setup has been largely detailed in [15]. The FTIR spectrometer is an Agilent Cary 670 FTIR. An optical setup is added to the sample compartment of the FTIR spectrometer. This setup has three functions. First, it redirects the IR beam from the spectrometer to the plasma where it goes back and forth, along the same optical path, thanks to a retro-reflector module. Second, it collimates the beam in the plasma zone via a set of two 2 by 2 mm² slits spaced 5 cm apart. These dimensions are essential to have a collimated beam over the 5 cm depth of the plasma at a spatial resolution of 2 mm. Finally, as the mercury-cadmium-telluride (MCT) IR detector is inside the spectrometer, this optical setup also redirects the returned beam to the IR detector. Another optical setup is installed between the spectrometer and the plasma reactor to scan the plasma. Both this setup and the retro-reflector module are installed on micrometric mounting plates to translate the IR beam over 10 mm. To perform measurements over a larger range, it is necessary to translate the discharge cell in the reactor.

2.2.2.Background.

In the present configuration, the IR beam passes through four KBr windows. Two are located on each side of the plasma to guide the gas from the inlet to the outlet, and the other two are located at the entrance and exit of the reactor. This configuration differs from the one previously used [15] which only had the windows at the entrance and the exit of the reactor. The four windows attenuate the signal but they are helpful because the reactor diameter is eight times larger than the plasma length: the optical path of the IR beam in the plasma reactor is twice 40 cm whereas the path in the plasma is twice 5 cm. In these conditions, even a small concentration of reactive molecules outside the plasma in the reactor considerably affects the measurement. Thus, the diffusion of reactive molecules out of the plasma should be avoided or at least minimized.
In a previous study [15], the plasma reactor was pumped until 5 Pa between each measure to evacuate molecules having diffused from the plasma zone to the rest of the reactor during the measurement. This method assumes that diffusion is the same during calibration and measurements. To be as reproducible as possible, calibration and plasma spectra were always done 30 seconds after starting the reactive gas injections. The discharge was turned on during this time to reach equilibrium. Since gas heat-up due to the plasma is lower than 10 K, the number of reactive molecules outside the plasma was assumed to be the same with and without the plasma. This questionable approximation is the reason why a better solution needs to be found.
The simplest solution to avoid gas diffusion is to close the plasma box. This is done by adding two IR-transparent KBr blades along the plasma zone to guide the gas flow from the injection to the exhaust system. In this configuration, molecules which otherwise would have diffused interact with the blades and can stick on them, increasing IR absorption. To take this into account, backgrounds are made

before and after each spectral acquisition, and the absorbance result is the mean of the values obtained with each background.

2.2.3.Calibration.

One of the advantages of the FTIR absorption method is that the absolute value of the density can be determined as long as a calibration curve is made. Whenever possible, this is done by making measurements using a known density of the measured species. Thus, the law that relates measured absorbance to species density is calculated and used to convert the absorbance measurements to gas density values. Thus, the first step is to establish this law. Figure 2 shows the results obtained for silane. Note the large data dispersion. However, the data can be divided into two groups, each fitted by a linear curve in agreement with the Beer-Lambert's law which establishes a linear relationship between gas species concentration and IR absorbance. The separation of these results, apparently obtained in the same conditions, into two groups has been assigned to room temperature variation. This variation is related to the dependence of molar absorptivity on temperature. Of course, this effect is avoided by performing measurements in a climate-controlled room. When this is not possible, the problem is avoided by making measurements with a low (30 ppm) and a high (67 ppm) concentration of SiH_4 just before each measurement to obtain the calibration curve.

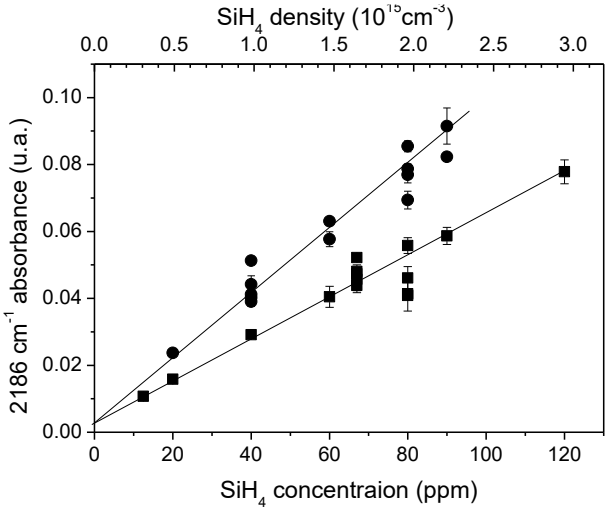

Figure 2 : Measured Si-H absorption as function of SiH_4 concentration in the gas phase for calibration curve. The difference between the two lines is due to room temperature variations.

To recap, the experimental procedure is as follows: first the calibration curve is determined from two sets of measurements made without plasma, the first set is composed of 3 measurements made with reactive gases in a concentration equal to that of the gas that will be injected in the plasma, and the second set is composed of 3 measurements made with a concentration close to the detection limit. Then, to determine the concentration in the plasma, 3 other independent measures are made with the plasma ON. A background is taken before and after each measurement. The gas concentration is determined using the mean of these 6 spectra (3 obtained on the first background and the other 3 on the second background). The standard deviation of the concentration determines the error on the measurements.

Another possible origin of measurement error is the gas heating by the plasma. However, in the conditions used in this work, the gas temperature variation induced by the plasma is less than 10 K which means less than 3% compared to the room temperature. This low temperature increase doesn't have any effect on the background as the background recorded plasma OFF and plasma ON are indistinguishable in the spectral range where there isn't absorption. The influence on the gas velocity is also negligible.

3. RESULTS

After reporting the analysis of a typical spectrum with and without plasma, we present and discuss the evolution with position for a given discharge power. These results will be compared to those obtained at different powers and with a modulated excitation to determine whether the energy is the dominant parameter. Finally, we look at the consequences of powder formation in the gas phase.

3.1. Typical FTIR spectra of a Ar–SiH_4–NH_3 glow-mode DBD

Figure 3 shows the IR spectra of the Ar–NH_3–SiH_4 (133 ppm/67 ppm) gaseous mixtures without (Figure 4a) and with (Figure 4b) plasma. Both spectra are recorded at the position corresponding to 7 mm after starting the plasma. In Figure 4a, the spectral signature of silane is observed through its asymmetric stretching mode vibration located at 2186 cm^{-1} and at the 907 cm^{-1} due to SiH_4 asymmetric bending [15]. Ammonia gives rise to components at 930 and 965 cm^{-1}, assigned to the symmetric bending mode of vibration of NH_3. This doubling is due to the fact that there are two equilibrium positions for the nitrogen atom at the two sides of the plane formed by the three hydrogen atoms (inversion doubling) [15]. Ammonia also produces several rotational bands which evidently surrounded 930 cm^{-1} and 965 cm^{-1} vibrational feature [15].

With the plasma, NH_3 absorption becomes too low to be processed. This is due to the presence of the KBr blades, as according to [15], NH_3 is measurable down to a concentration of 40 ppm when the gas is pumped between each measurement. However, SiH_4 density is easily measurable from 2186 cm^{-1} absorbance. There is no new absorption resulting from plasma chemistry. The densities of reactive gas fragments and secondary products are too low to be measured by FTIR, so in the following, it is the evolution of SiH_4 density as a function of the position and energy that is presented.

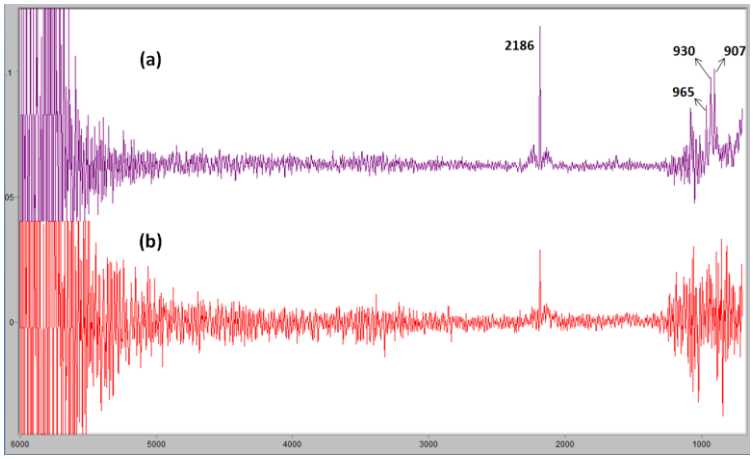

Figure 3 : Spectra of an Ar–NH_3–SiH_4 mixture a) without plasma and b) with plasma.

3.2. Silane consumption as a function of position in the plasma

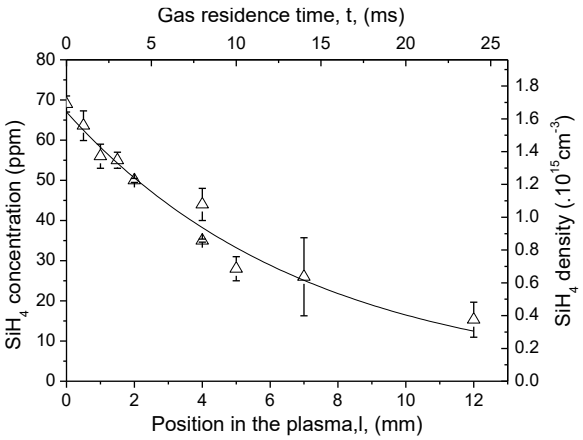

Figure 4: Silane concentration and density as a function of position of the IR beam in the plasma and the associated time for a power density of 85 mW/cm³

Figure 4 shows silane concentration and density as a function of position, *l*, in the plasma from 0 to 12 mm. Discharge power, *P*, is set at 127 mW, i.e. 85 mW/cm³. For the purpose of comparison with results from other works, the position is also converted into a gas residence time, *t*, in the plasma defined as: $t = l.S/F = 2.l$ where *F* is gas flow (3 L/min) and *S* is plasma cross-section in the direction perpendicular to gas flow (50 by 2 mm²). The silane decrease concentration with position or time is well fitted by the exponential law of equations 2 and 3. The characteristic length and time are $l_0 = 7$ mm or $\tau_0 = 14$ ms, which means that all the silane would be dissociated if the plasma length is more than 5 l_0 (35 mm) or the gas residence time is longer than 5 τ_0 (70 ms).

$$[SiH_4](\text{ppm}) = 67\exp(-\frac{l(\text{mm})}{7}) \qquad \textbf{Equation 2}$$

$$[SiH_4](\text{ppm}) = 67\exp(-\frac{t(\text{ms})}{14}) \qquad \textbf{Equation 3}$$

3.3. Effect of energy on silane dissociation

For a constant discharge power, *P*, the position or gas residence time is related to an energy "seen" by the chemical species between their injection in the plasma and the measurement point, *E (E=P.t)*. To determine whether this energy is the parameter controlling silane dissociation, measurements were made as a function of discharge power for the 5 and 6 mm positions.

Silane concentration as a function of energy is presented in Figure 5. Open triangles are the results previously presented, i.e. measurements made as a function of position for the 85 mW/cm³ power density. Stars correspond to measurements done at a fixed position for different voltage amplitudes and thus different power values ranging from 60 to 300 mW. White stars are points measured at 5 mm and black stars are points measured at 6 mm.

$$[SiH_4](\text{ppm}) = 67\exp(-\frac{E(J)}{0.0019}) \qquad \textbf{Equation 4}$$

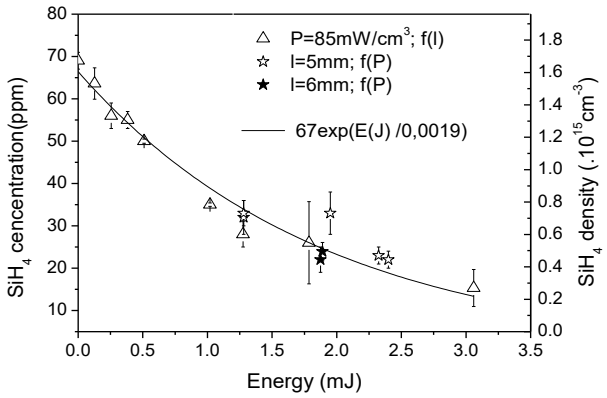

Figure 5 : Silane concentration as a function of energy, △: data measured as a function of position for a power density of 85 mW/cm³ (figure 7). Stars are datasets measured as a function of discharge power ☆at 5 mm and ★ at 6 mm .

All points are aligned on an exponential law with E_0= 1.9 mJ according to equation 4. This exponential fit suggests that, in our conditions, 10 mJ is enough to dissociate 67 ppm of silane, i.e. 150 µJ to dissociate one ppm of silane or $6.09.10^{-18}$ J: 38 eV to dissociate one hydrogen atom from one molecule of silane. The fact that for a given initial concentration of silane, the local concentration is determined by the energy that the silane molecules have "seen" suggests that precursor dissociation is limited by discharge power and that the rather low power of the glow DBD can be compensated for by a larger plasma zone along the direction of the gas flow.

According to the literature, plasma modulation is a good solution for increasing the quality of thin films realized with a DBD [19]. Thus it is of interest to study the consequence of this modulation on the FTIR spectra and on silane dissociation.

3.4. Effect of 50 kHz power modulation

A square signal is superimposed over the 50 kHz excitation to modulate the voltage applied to the electrodes. This modulated signal is composed of a time ON, T_{on}, when the original sinusoidal voltage is applied, and a time OFF, T_{off}, where no voltage is applied and so the plasma is off. For a 5 ms period defined as $T_{on} + T_{off}$, two duty cycle (*DC*) defined as $DC = T_{on}/(T_{on}+T_{off})$ were used: 0.3 or 0.6, meaning that the plasma is respectively ON for 1.5 or 3 ms and OFF for 3.5 or 2 ms. These measurements were done at the 5 mm position.

Figure 6 regroups all previous data points plus the new one represented by open and black circle. It clearly shows that the decrease in silane concentration induced by modulated plasma is well described by equation 4. SiH_4 dissociation depends solely on plasma energy, i.e. only negligible chemistry occurs during T_{off}. At first look, this result could appear surprising given that in a GDBD, electrons and metastable densities are quite comparable [19] and SiH_4 is rather efficiently dissociated by the metastable $Ar(^3P_2)$.

$Ar(_3P^2) + 2Ar \rightarrow Ar_2^* + Ar$	K_4=2.45.10^{-13} cm^3/s	**Equation 5**
$Ar(_3P^2) + SiH_4 \rightarrow SiH_2 + 2H + Ar$	K_5=4.6.10^{-10} cm^3/s	**Equation 6**
$Ar(_3P^2) + SiH_4 \rightarrow SiH_3 + H + Ar$	K_6=1.4.10^{-10} cm^3/s	**Equation 7**

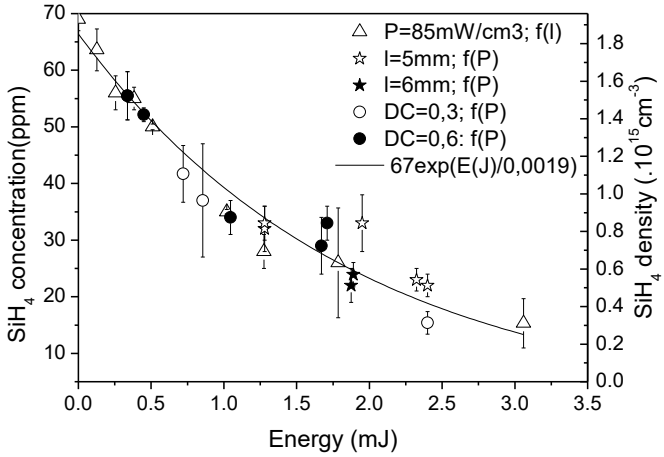

Figure 6 : Silane concentration as a function of energy in a GDBD. ○ were measured with a modulated plasma with *DC* = 0.3 and ● for a *DC* = 0.6

SiH_4 dissociation by Ar metastable is in competition with Ar_2 formation. At atmospheric pressure for 67 ppm of SiH_4, the respective contribution of each reaction is 78% for Ar_2 formation and 13% for SiH_4 dissociation. Thus $Ar(^3P_2)$ contributes to SiH_4 dissociation. However, $Ar(^3P_2)$ has a short life-time: equations 4 to 6 lead to a lifetime of 120 ns. It is mainly converted to Ar_2 which also has a rather short life-time due to radiative de-excitation leading to VUV emission. Thus species able to dissociate SiH_4 have a short life-time. As GDBD is a pulsed discharge, this time should be compared to the time between two discharges. According to Figure 7, which presents the discharge current, the typical duration of the discharge is 2 µs and the time between two discharges is about 8 µs. During that time window, there is still energy in the plasma, including electrons and ions, but their density and energy decreases by a factor 10 of more than. As only energetic species created by the discharge (electrons, Ar*, Ar_2) and having a short life-time are able to dissociate SiH_4, the pulsed nature of GDBD has the same consequences as an excitation modulation. Dissociation mainly occurs during the discharge, and the modulation at a time-scale of milliseconds has no effect.

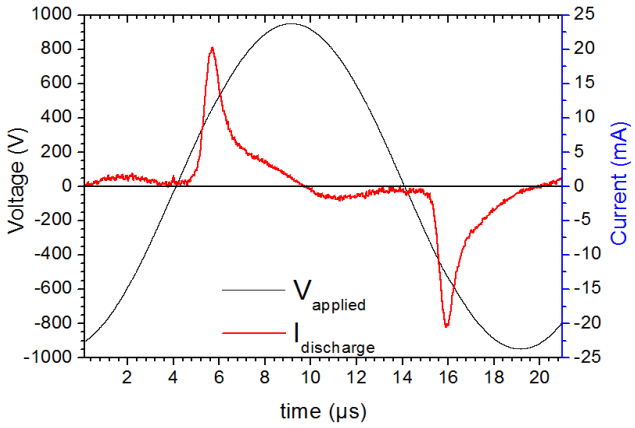

Figure 7 : Time resolved voltage and current signals of glow DBD (Ar–NH_3–SiH_4). P = 375 mW/cm^3

3.5. Effect of powder formation

One of the limitations of atmospheric-pressure plasma-enhanced chemical vapor deposition (AP-PECVD) is powder formation. This phenomenon is enhanced in collisional plasma when the precursor gases or vapors are highly reactive, as is the case with SiH_4 [20], and it is always observed when

microdischarges develop due to the high local density of energetic species[21]. Here, silane-based powders are made by turning the discharge into filamentary mode or by injecting a small amount of oxygen which enhances silane dissociation to form radicals that react with SiH_4[21].
Whatever the conditions, the spectra are similar and there is no other quantifiable absorption than that of SiH. SiH vibration depends on its environment: the absorption peak of SiH in SiH_4 is at 2186 cm^{-1} and the absorption peak of SiH in SiH_3 is at 2183cm^{-1}. To be sure that SiH absorption can be related to SiH_4, figure 8 compares SiH absorption peaks with and without powder. Surprisingly, the absorption peaks are quite similar, showing that even when powders are formed, SiH absorption is well related to SiH_4 concentration.

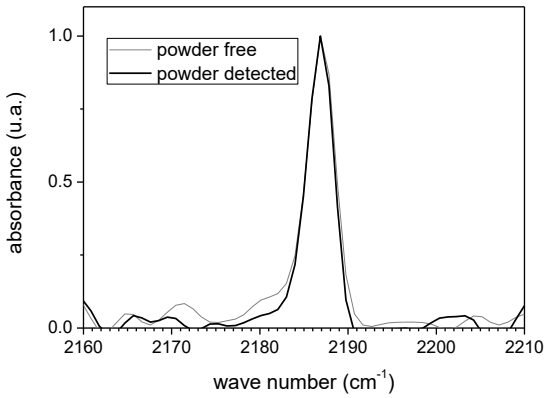

Figure 8 : Comparison of the spectra with and without powders in SiH_4 vibrations region.

Figure 9 compares SiH_4 concentration as a function of energy in powder-forming and non-powder-forming conditions. Powder formation was checked by observing the diffusing surface coating. To facilitate readability, only data points made as a function of position are reported in order to tease out results without powders. Measurement corresponding to the black square was made with a filamentary discharge obtained by sufficiently increasing the voltage to switch from glow DBD to filamentary discharge. In this case, the voltage applied to the electrodes switch from 1.8 kVcc (mean power density of 85 mW/cm^3) for the glow DBD mode to 2.6 kVcc (mean power density of 2.5 W/cm^3) for the filamentary mode. The open square have been obtained with a small addition of oxygen. Figure 9 clearly shows that the concentration of SiH_4 remains higher when powders are formed. According to the exponential fit of data obtained with powders, SiH_4 decay is more than 4 times slower when powders are formed. At a 50 kHz excitation, a large fraction of powders with a diameter larger than 20 nm are trapped in the gas. However, absorbing Si-H are not part of the powders, as in powder form, SiH_4 should be transformed into SiH_x with $x<4$. This lower SiH_4 dissociation could be related to the decrease of electron density due to electrons being trapped on the powders [23] and thus no longer available to dissociate SiH_4.

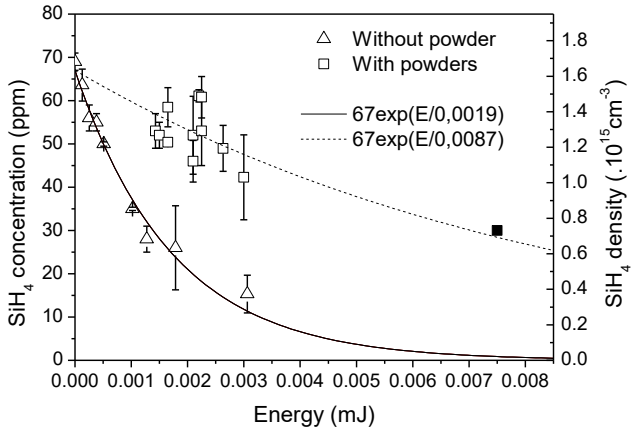

Figure 9 : Comparison of silane concentration as a function of energy, Δ without powder formation in the plasma, with powder formation, □ due to oxygen, and ■ due to microdischarges.

4. CONCLUSION

This research used FTIR absorption spectroscopy to study the evolution of an Ar–NH_3–SiH_4 mixture in a plane-plane DBD of 2 mm gap. Plasma configuration and measurement procedure were optimized to increase accuracy while minimizing measurement times. Measurements were done by injecting 133 ppm of NH_3 and 67 ppm of SiH_4. Whatever the conditions, the absolute density of SiH_4 is easily measured with a 2 by 2 mm² IR beam having a 10 cm path length in the plasma. The N-H vibration of NH_3 is observable but non-quantifiable. No reaction products were detected.

SiH_4 dissociation has been studied as a function of position in the plasma along the gas flow from 0 to 12 mm. Power has been varied from 60 to 300 mW by changing the voltage amplitude of the 50 kHz excitation. Power has also been modulated with a square signal of 5 ms period and duty cycles of 0.3 or 0.6. Whatever the conditions, silane concentration decreases exponentially with the energy injected in the plasma from the gas inlet to the measurement point. All the measurements are fitted by the same exponential decay as a function of energy as long as there is no powder formation in the plasma. The decay corresponds to 42eV per SiH_4 molecule dissociated. The absence of modulation effect is explained by two points (i) The GDBD is composed of pulsed discharges with duration of only 2 µs, lower than the 10 µs of half a period of the electrical signal, (ii) silane is only dissociated by energetic species and the life time of energetic species is short compared to the time between two discharges. Thus, silane concentration is a direct function of energy. Silane dissociation rate is lower in presence of powder than in absence of powder. A possible explanation is the fact that electrons get trapped on the powders and are no longer available to dissociate SiH_4.

FTIR absorption spectroscopy of Ar-SiH_4-NH_3 mixtures with low concentration of reactive gases allows characterizing SiH_4 dissociation. This could have been done with a laser diode. However, this first insight on FTIR characterization of DBD clearly shows the possibilities for more complex precursors like organosilicon compounds.

Acknowledgements

This work was supported by the French Environment and Energy Management Agency (ADEME) and "Air Liquide"

REFERENCES

[1] Kogelschatz U, 2003. Dielectric-barrier discharges: Their history, discharge physics, and industrial applications. *Plasma Chemistry and Plasma Processing*, **23**, No. 1.

[2] Sladek REJ, Filoche SK, Sissons CH, and Stoffels E, 2007. *Letters in Applied Microbiology*, **45**, 318.

[3] Topala I, Asandulesa M, Spridon D & Dumitrascu N, 2009. *IEEE Transactions on Plasma Science* **37**, 946.

[4] Wang K, Li J, Ren C, Wang D & Wang Y, 2008. *Plasma Science and Technology* **10**, 433

[5] Chevallier P, Castonguay M, Turgeon S, Dubrulle N, Mantovani D, McBreen PH, Wittmann J-C, and Laroche G, 2001. *J. Phys. Chem.* B **105**, 12490.

[6] Borcia G, Anderson CA & Brown NMD, 2004. *Applied Surface Science* **225**, 186.

[7] Weltman K D, Kindel E, Von Woedtke T., Haehnel M, Stieber M and Brandenburg R , 2010, *Pure and applied chemistry*, 82(6) 1223-1237

[8] Bardos L & Barankova H, 2005. *Journal of Vacuum Science & Technology* A **23**, 933.

[9] Choi J, Iza F, Do HJ, Lee JK & Cho MH, 2009. *Plasma Sources Science & Technology* **18.**

[10] Wang C, Koirala SP, Scherrer ST, Duan Y & Winstead CB, 2004. Diode laser microwave induced plasma cavity ringdown spectrometer: Performance and perspective. *Rev. Sci. Instrum.* **75**, 1305.

[11] Mercier X, Therssen E, Pauwels JF & Desgroux P, 2005. *Proceedings of the Combustion Institute* **30**, 1655.

[12] Moreau C, Therssen E, Desgroux P, Pauwels JF, Chapput A & Barj M, 2003. *Applied Physics B-Lasers and Optics* **76**, 597.

[13] Stancu GD, Kaddouri F, Lacoste DA & Laux CO, 2010. Atmospheric pressure plasma diagnostics by OES, CRDS and TALIF. *J. Phys. D: Appl. Phys*. **43** 124002.

[14] Röpcke J, Lombardi G, Rousseau A & Davies P B, 2006. Application of mid-infrared tuneable diode laser absorption spectroscopy to plasma diagnostics: a review. *Plasma Sources Sci. Technol.* **15** S148.

[15] Laroche G, Vallade J, Bazinette R, Van Nijnatten P, Hernandez E, Hernandez G & Massines F, 2012. Fourier transformed infrared absorption spectroscopy characterization of gaseous atmospheric pressure plasmas with 2 mm spatial resolution. *Rev. Sci. Instrum*. **83**, 103508.

[16] Vallade J, Pouliquen S, Lecouvreur P, Bazinette R, Hernandez E, Quoizola S, Massines F, 2012, "a-SiNx:H Antireflective And Passivation Layer Deposited By Atmospheric Pressure Plasma" *Energie Procedia*, **27**, 365-371

[17] Herzberg G, 1945. Molecular Spectra and Molecular Structure - Spectra of Diatomic Molecules. *Van Nostrand Company, Inc., New York*, Vol. 2.

[18] Radzig AA, Smirnov BM, 1985, Reference Data on Atoms, Molecules and Ions, *Springer-Verlag*, Berlin Heidelberg New York Tokyo.

[19] Massines F, Sarra-Bournet C, Fanelli F, Naudé N & Gherardi N, 2012. Atmospheric pressure low temperature direct plasma technology: status and challenges for thin film deposition. *Plasma Processes Polym.* **9** (11-12),1041–1073.

[20] Boscher ND, Choquet P, Duday D & Verdier S, 2010. *Plasma Processes Polym*. **7**, 163.

[21] Massines F, Gherardi N, Naudé N & Ségur P, 2005. Glow and Townsend dielectric barrier discharges in various atmospheres and particle formation. *Plasma Physics and Controlled Fusion*, **47** B577-B588.

[22] Bouchoule A, 1999. Dusty plasmas: physics, chemistry, and technological impacts in plasma processing., *JohnWiley &sons LtD.*

[23] N. Jidenko, C. Jimenez, F. Massines and J.P. Borra 2007. Nano-particle size-dependent charging and electro-deposition in dielectric barrier discharges at atmospheric pressure for thin SiOx film deposition. *J. Phys. D: Appl. Phys.* **40**